Blackbody Excitation of an Atom Controlled by a Tunable Cavity

K. S. Lai* and E. A. Hinds

Sussex Centre for Optical and Atomic Physics, University of Sussex, Falmer, Brighton BN1 9QH, United Kingdom

(Received 13 March 1998)

We have used a gold cavity to control the blackbody spectrum and hence to alter thermal excitation of a Rydberg atom. We suppress the cesium transition $13S$-$13P$ or $14S$-$14P$ when the cavity width is less than half the transition wavelength, 37 or 50 μm. Our measurements resolve the fine structure to a few percent. The experimental curves can be understood by summing multiple reflections of the atomic dipole in the walls of the cavity. Changing the temperature shows explicitly that the excitation rates are indeed proportional to the number of photons per mode of the blackbody field. [S0031-9007(98)07187-7]

PACS numbers: 42.50.Ct, 32.70.Jz, 32.80.Rm

In cavity quantum electrodynamics (QED) the radiative properties of an atom are modified when cavity walls impose a boundary condition on the electromagnetic field [1–3]. Experiments on the low-temperature limit of cavity QED have shown that spontaneous emission rates are altered [4–6] and that atomic levels are shifted [7–9]. By comparison, the effects of a cavity at nonzero temperature have hardly been studied. To the best of our knowledge there has been only one previous experiment on finite temperature effects in a confined environment [10], in which the rate of the $29D$-$30P$ transition in Cs was altered between capacitor plates spaced 3 mm apart. It is already well established that blackbody radiation strongly influences the lifetimes and energy levels of Rydberg atoms in free space [11–15], and now calculations by Nakajima *et al.* [16] predict striking modifications to both when the atoms are enclosed in a parallel plate cavity. We have observed some of these in the laboratory. Here we describe a detailed, quantitative study of cavity QED control over blackbody-induced population transfer, using the Cs transitions $13S$-$13P_{1/2,3/2}$ and $14S$-$14P_{1/2,3/2}$. We have demonstrated for the first time the temperature dependence and the fine structure splitting of the effect.

Consider an S-P transition induced at a rate γ_0 in free space by blackbody radiation of wavelength λ. Because the S state is isotropic, $\frac{1}{3}$ of the rate is excited by each of the three independent polarizations. In a parallel-plate waveguide of width L at the same temperature, the transition rate is modified because of the boundary condition and one expects [1]

$$\gamma_{\parallel} = \frac{2}{3}\,\gamma_0 \sum_{n=0}^{n_{\max}} \frac{3\lambda}{4L}\left[1 + \left(\frac{n\lambda}{2L}\right)^2\right] \sin^2\left(\frac{n\pi z}{L}\right),$$

$$\gamma_{\perp} = \frac{1}{3}\,\gamma_0 \left\{\frac{3\lambda}{4L} + \sum_{n=1}^{n_{\max}} \frac{3\lambda}{2L}\left[1 - \left(\frac{n\lambda}{2L}\right)^2\right] \cos^2\left(\frac{n\pi z}{L}\right)\right\}, \tag{1}$$

where $n_{\max}$ is the integer part of $2L/\lambda$ and z is the distance from one plate. When the width is just less than $\lambda/2$, the field parallel to the plates is cut off, leaving a transition rate $0.5\gamma_0$ due to the perpendicular field. At $L = \lambda/2$ this jumps discontinuously by $2\gamma_0 \sin^2(\pi z/L)$ with the appearance of the lowest parallel mode, giving a total rate of $1.5\gamma_0$ when averaged over all positions z. Since the reflectivity of real plates never quite reaches unity, the step is in fact continuous and the ratio of transition rates above and below the cutoff is less than 3. For example, with a reflectivity of 0.99, calculations based on the summation of multiple reflections [17] show that the ratio of excitation rates is only 2.7 and the step has a width of approximately $3 \times 10^{-3}\lambda$. Such steps are the subject of the measurements reported here.

Our experiment uses a horizontal atomic beam of Cs effusing through a 50 μm wide slit from a 100 °C oven into a turbo-pumped source chamber. The main vacuum chamber is ion-pumped to 5×10^{-8} Torr, and liquid nitrogen cooled surfaces minimize the background Cs vapor. At 20 cm from the oven, the beam ($\sim 10^{11}$ atom cm^{-2} s^{-1}) enters a parallel plate cavity (Fig. 1) formed by glass blocks 3 cm high and 8 mm along the beam. Stray fields are reduced by a coating of indium tin oxide (ITO), which conducts at low frequency but is transparent to visible and near-ir light. One block is rotated in a mirror mount to

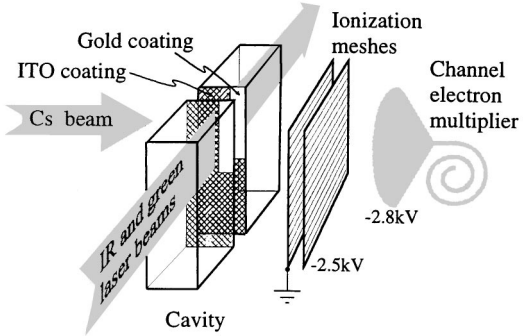

FIG. 1. Schematic diagram of apparatus. A beam of cesium is collimated by two ITO-coated glass blocks and promoted by laser light to $13S$ or $14S$. The atoms fly into a gold cavity where blackbody radiation excites them to higher-lying states. After leaving the cavity, the thermally excited atoms are field ionized and counted.

make the two faces parallel. The other is piezoelectrically translated to scan the cavity width by 50 μm while maintaining parallelism within a few microradians, as monitored by optical Fabry-Perot fringes. The reflectivity of ITO in the 10–100 μm wavelength range is below 80%, not high enough to control the blackbody field as required for our experiment. We therefore make a high-Q cavity ($Q \sim 10^3$) at the exit end of the parallel plate structure (Fig. 1) by coating an additional layer of gold 6 mm high, 1.3 mm along the beam, and 200 nm thick. This is not degraded by Cs deposition because the beam intensity is low and the angle of incidence oblique; less than 1% of a monolayer is deposited in a day.

Just before the cesium atoms enter the gold cavity, we excite them either to 13S or to 14S by the doubly resonant transition 6S-6P-nS. The first step is driven by 852 nm light from a grating-stabilized cw diode laser [18], while the second step uses light at 546 nm (13S) or 538 nm (14S) from a CR699 ring dye laser. Both lasers are locked to signals from an auxiliary atomic beam, allowing the atom excitation rate to be held constant within a few percent for periods of several hours. The two laser beams are overlapped on a dichroic splitter and focused to a line approximately 200 μm wide (along the atomic beam direction) and 5 mm high, just outside the gold plates. The first-order Doppler effect is suppressed by ensuring that the light is perpendicular to the parallel plate cavity surfaces. After traversing the gold cavity, the atomic beam passes through the first of two fine copper meshes, spaced by approximately 0.5 mm, where an electric field ionizes atoms that are highly excited. The ions are then detected by a channel electron multiplier with a count rate of ~100 kHz. A small frequency scan of the green laser produces an excitation spectrum which exhibits the Autler-Townes splitting when the two light beams are well overlapped and the infrared intensity is high enough. We reduce the infrared power to ~1 mW, where the excitation peak is ~15 MHz wide and there is some broadening but no splitting. The power in the green excitation beam is ~20 mW.

Our detector is sensitive only to atoms that are sufficiently highly excited. According to the saddle-point model, the field required to ionize nS is $3 \times 10^{10}(n - \delta_s)^{-4}$ V/m, where the quantum defect δ_s is 4.0 in Cs. With our ionizing field at 5 MV/m, we should therefore detect states down to 13S, but not lower. We checked this by exciting to 13S at a distance L before the detector (with no cavity). The points in Fig. 2 show the excited atom signal versus L, normalized to the signal measured at $L = 4.1$ mm. These points are incompatible with curve (*a*), the decrease of 13S population based on the known spontaneous 13S lifetime of 0.754(35) μs [19]. Our signal decays much more slowly because the blackbody radiation transfers atoms into higher-lying Rydberg states whose lifetimes are longer. We have computed the evolution of the Rydberg state populations at room temperature by brute force integration of the 42 coupled rate equations connecting states 11S-20S, 10P-20P, 9D-19D, and 7F-16F. (The dipole matrix elements are calculated from Edmonds *et al.* [20]; the total lifetimes are taken from Ref. [19].) In this way we predict the decay curve as a function of L after integrating over the velocity distribution of the atomic beam to convert the elapsed time to a distance. The line marked (*b*) in Fig. 2 shows the result of this calculation when we assume that the ionizer detects all states down to 14S, while the lower line (*c*) is for detection down to 13S. The two curves bracket the data very satisfactorily, indicating that we have a good understanding of the blackbody-induced population transfer and of our detector. This is confirmed by similar experiments starting in the 14S state and by measurements using a range of weaker ionizing fields down to 2 MV/m.

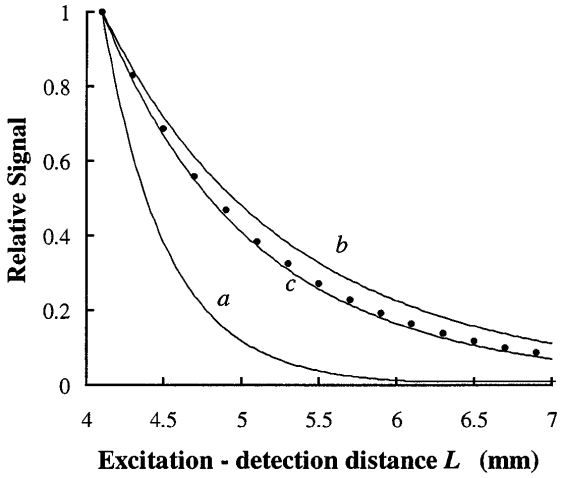

FIG. 2. Excited atom signal versus L following excitation to the 13S state. Our measurements (dots) are incompatible with spontaneous decay (*a*) of 13S state. Curves *b* and *c* are calculated Rydberg signals, taking into account thermal excitations and assuming detection of all states above 14S (*b*) or 13S (*c*). Consistency of these with our data indicates a good understanding of the blackbody-induced population transfer and of our detector.

Of all the excitations out of 13S, the transition to 13P has the strongest matrix element and its wavelength $\lambda_{13} = 74.5$ μm is close to the peak of the room-temperature blackbody spectrum. In free space at 20 °C, we calculate that 94% of all upward transitions out of 13S go first to 13P, which acts as a gateway giving access to the higher states. Nevertheless, only 70% of the excited atom signal is due to these atoms. The other 30% is from atoms excited via higher-lying states, which are less liable to decay subsequently below the detection threshold. As the 13S-13P transition rate is varied in our model between 0 and $2\gamma_0$, we find that the ionization signal varies linearly, reflecting the fact that the thermal excitation rate is much slower than the downward decay rate.

In order to study the cavity modification of the 13S-13P rate, we excited the atomic beam to 13S with the lasers placed immediately upstream from the gold cavity, as shown in Fig. 1. After a brief flight of typically 100 μm

($\sim$0.4 μs) in the ITO region, the atoms pass into the gold cavity whose highly reflecting walls are intended to affect the spectral and spatial distribution of the blackbody field. In particular, the $13S$-$13P$ thermal excitation rate is expected to decrease abruptly by a factor slightly less than 3 when the cavity width is reduced below $\lambda_{13}/2$. The points in Fig. 3 show the Rydberg atom signal versus the width of the gold cavity. This clearly exhibits two sudden changes in the excitation probability and demonstrates the cavity cutoff of the atom-blackbody interaction. The upper step is due to inhibition of the $13S$-$13P_{1/2}$ transition and is centered at a cavity width of 38.5(5) μm, while the second one, associated with $13S$-$13P_{3/2}$ transitions, is at 36.1(5) μm. The step heights are in the ratio 1:2, reflecting the statistical weight ratio of the two transitions. The separation between the steps is 2.39(4) μm, implying a $13P$ fine structure splitting of 257(7) GHz in good agreement with the value 255(2) GHz known from optical spectroscopy [21]. Hence, our experiment could alternatively be viewed as an unusual spectroscopic method in which blackbody radiation is used as a far infrared source to determine the fine structure splitting by a direct length measurement. Although the absolute cavity width is uncertain by ± 0.5 μm, this width difference is accurately calibrated by monitoring the transmission of the infrared light used to excite the atoms. The 8% reflectivity of the ITO at 852 nm gave fringes of quite adequate visibility for this purpose.

Two important systematic corrections have been made to the data shown in Fig. 3. First, because the Fabry-Perot resonances modulate the intensity of the infrared light, the excitation probability has a noticeable oscillation as the cavity width is scanned. This is removed numerically by our LABVIEW data acquisition software using a notch filter centered on a spatial period of 426 nm. Second, the detected signal decreases as the cavity width w is reduced, simply because the geometrical transmission $T(w)$ is smaller for a narrower cavity. In order to convert the result to one of constant total beam intensity, we scale the signal by the known transmission ratio $T(w_{\max})/T(w)$, where $w_{\max} = 40.5$ μm is the largest width in the scan.

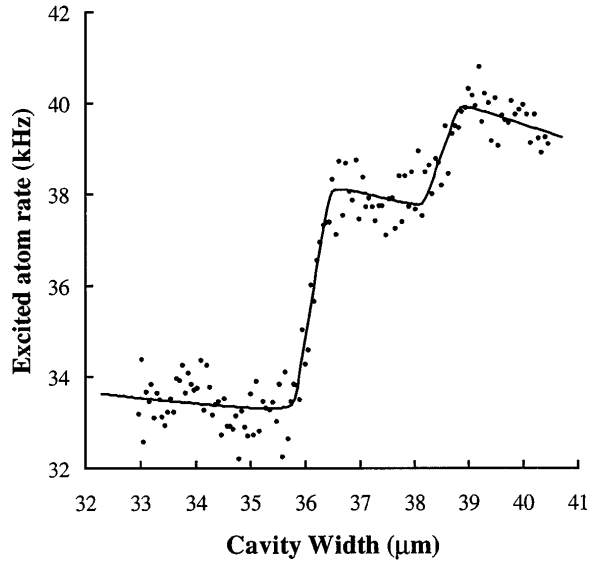

FIG. 3. Signal following $13S$ excitation versus width of the gold cavity. Dots are experimental, and the line is a fit. The measurements show a sharp increase of the $13S$-$13P_{3/2}$ excitation rate at a width of 36.1(5) μm and a second step of half the size at 38.5(5) μm due to the $13S$-$13P_{1/2}$ transition.

The steps are 0.7 μm wide. Part of this is due to the angle between the plates, which was adjusted for experimental convenience to give two infrared fringes per cm of height and therefore accounts for approximately 0.4 μm of the step width. The remainder is due to the imperfect reflectivity of the gold surface. In order to check the shape of our excitation curve in detail, we have made a least-squares fit to a simple numerical model indicated by the solid line in Fig. 3. In this model we adjust the zero of cavity width, the constant background excitation rate, the reflectivity of the mirrors, and the atomic beam intensity. The $13S$-$13P$ transition rate is calculated by summing multiple reflections in the cavity [17] and convolving the result over the 0.4 μm range of cavity widths. This model agrees well with the data, confirming that the steps are due to cavity control of the blackbody field. Our fit indicates that the mirrors have reflectivity $(99.6^{+0.1}_{-0.4})\%$, a result that is consistent with the expected 99.7% reflectivity for gold in this wavelength range [22]. The background rate determined in this way was 29 kHz. Approximately half of it was due to blackbody excitation at shorter wavelength to higher states than $13P$, while the other half results from free-space excitation in the 100 μm flight region preceding the cavity. We have checked that we understand the latter contribution by changing the distance from the excitation lasers to the cavity entrance and observing the expected variation in the background. We have repeated the experiment without the gold cavity by lowering the laser beams to the region without any gold coating (see Fig. 1), and we find that the two sharp steps are replaced by a smooth, weak variation. This is to be expected because of the low reflectivity, $\leq$80%, of the indium tin oxide surfaces at the transition wavelengths [23]. We have also excited atoms to the $14S$ state instead of $13S$. In that case there was no variation of the excited atom signal (except for the trivial geometrical one) when the gold cavity width was scanned between 35 and 40 μm. However, steps reappeared, as shown in Fig. 4, when the cavity width was increased to $L \approx 50$ μm, which is half the transition wavelength for $14S$-$14P$.

In order to confirm the role of the blackbody field, we measured the excitation signal out of $14S$ at two different temperatures, 296 and 448 K, with results shown in Fig. 4. For this comparison, we were particularly careful to keep the intensities of the atomic and laser beams constant so that the absolute size of the excitation signal reliably measures the intensity of the blackbody radiation. After such a large temperature change, the cavity must be realigned, and this introduces an unknown offset in the

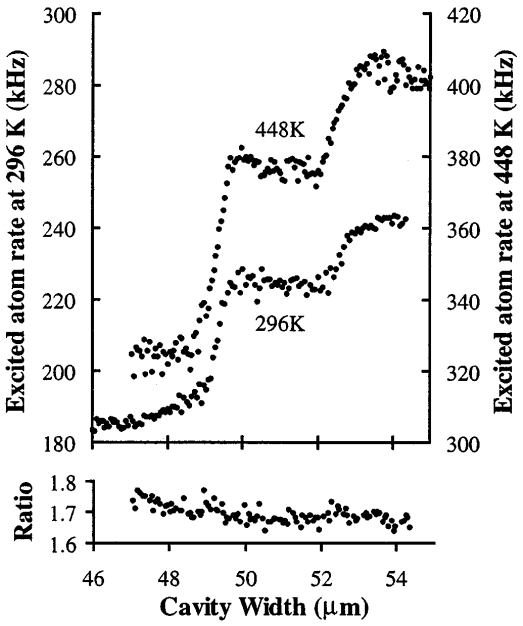

FIG. 4. Upper graph: signals following 14S excitation versus width of the gold cavity at two different temperatures (note the two ordinates). The steps demonstrate cavity control of the 14S-14$P_{3/2}$ and 14S-14$P_{1/2}$ transitions. The lower graph shows that the ratio of the two signals is constant and close to 1.64, the ratio of the number of photons per mode in the blackbody fields at these two temperatures.

absolute cavity width, which we have adjusted in Fig. 4 to make the high and low temperature steps coincide. We see that the two curves are the same except for the greatly increased rate of excitation in the hotter experiment (note the two different axes). A thermal excitation rate should be proportional to the mean number of blackbody photons per mode $[\exp(hc/\lambda kT) - 1]^{-1}$. At the two temperatures in Fig. 4, the ratio of photon numbers for the 100 μm wavelength of the 14S-14P transition is 1.64, to be compared with the experimental ratio of excitation rates plotted at the bottom of Fig. 4. The measured ratio is almost constant, and only slightly higher than 1.64. This is consistent with our view that the excited atom rate is due mainly to blackbody excitation of the 14S-14P transition with a minor contribution to the background from shorter wavelength transitions.

This experiment demonstrates how a cavity can control the blackbody spectrum and hence can alter the thermal excitation rate of an atom. First, we showed that the signal in our detector is due to thermal excitation of the atoms from their initial 13S or 14S state to higher-lying levels, mostly via 13P or 14P. Next we showed that the excitation rate could be strongly suppressed inside a microscopic parallel plate gold cavity when the cavity width was reduced below the fundamental cutoff. In each case we saw two steps in the excitation rate corresponding to the two fine structure components nS-$nP_{1/2}$ and nS-$nP_{3/2}$, whose separation we could measure with a few percent accuracy. The experimental curves were well described by a simple theory in which the excitation rate is calculated by summing the multiple reflections of the atomic dipole in the walls of the cavity. Finally, we changed the temperature of the cavity and showed that the measured excitation rates were indeed proportional to the number of photons per mode of the blackbody field, as one would expect for thermal excitation.

The authors thank Malcolm Boshier and Gabriel Barton for many productive discussions. Matthew Key, Alan Butler, and John Osborne provided technical assistance. This work was funded by the NSF, the UK EPSRC, the EU, and Sussex University.

*Also at Sloane Physics Laboratory, Yale University, 217 Prospect Street, New Haven, CT 06520.

[1] E. A. Hinds, Adv. At. Mol. Opt. Phys. **28**, 237 (1991).
[2] *Cavity QED*, edited by P. R. Berman (Academic Press, New York, 1991).
[3] G. Barton, Proc. R. Soc. London A **410**, 141 (1987); **410**, 175 (1987).
[4] P. Goy *et al.*, Phys. Rev. Lett. **50**, 1903 (1983).
[5] R. G. Hulet, E. S. Hilfer, and D. Kleppner, Phys. Rev. Lett. **55**, 2137 (1985).
[6] W. Jhe *et al.*, Phys. Rev. Lett. **58**, 666 (1987).
[7] V. Sandoghdar *et al.*, Phys. Rev. Lett. **68**, 3432 (1992).
[8] C. I. Sukenik *et al.*, Phys. Rev. Lett. **70**, 560 (1993).
[9] D. J. Heinzen and M. S. Feld, Phys. Rev. Lett. **59**, 2623 (1987).
[10] A. G. Vaidyanathan, W. P. Spencer, and D. Kleppner, Phys. Rev. Lett. **47**, 1592 (1981).
[11] T. F. Gallagher and W. E. Cooke, Phys. Rev. Lett. **42**, 835 (1979).
[12] W. E. Cooke and T. F. Gallagher, Phys. Rev. A **21**, 588 (1980).
[13] J. W. Farley and W. H. Wing, Phys. Rev. A **23**, 2397 (1981).
[14] L. Hollberg and J. L. Hall, Phys. Rev. Lett. **53**, 230 (1984).
[15] G. Barton, J. Phys. B **20**, 879 (1987); G. Barton, in *Spectrum of Atomic Hydrogen*, edited by G. Series (World Scientific, Singapore, 1988), p. 469.
[16] T. Nakajima *et al.*, Phys. Rev. A **56**, 5100 (1997).
[17] E. A. Hinds, Chap. 1 in Ref. [2], Eqs. (10), (18), and (19).
[18] M. G. Boshier *et al.*, Opt. Commun. **85**, 355 (1991).
[19] C. E. Theodosiou, Phys. Rev. A **30**, 2881 (1984).
[20] A. R. Edmonds *et al.*, J. Phys. B **12**, 2781 (1979).
[21] C. J. Lorenzen and K. Niemax, J. Quant. Spectrosc. Radiat. Transfer **22**, 247 (1979).
[22] M. A. Ordal *et al.*, Appl. Opt. **26**, 744 (1987).
[23] I. Hamberg and C. G. Granqvist, J. Appl. Phys. **60**, R123 (1986).